Lamellar Morphology by Small-Angle X-ray Scattering Measurements in Some Perfluorinated Copolymers of Tetrafluoroethylene

Antonio Marigo, Carla Marega, and Roberto Zannetti*

Dipartimento di Chimica Inorganica, Metallorganica ed Analitica dell'Università, via Loredan, 4, 35131 Padova, Italy

Giuseppe Ajroldi

AUSIMONT S.p.A., Bollate (Milano), Italy

Received June 9, 1995; Revised Manuscript Received December 20, 1995[⊗]

ABSTRACT: Some samples of tetrafluoroethylene copolymers, containing perfluoropropyl vinyl ether, perfluoromethyl vinyl ether, and hexafluoropropene, were studied by small-angle X-ray scattering in order to investigate the correlation among the crystalline lamellar thickness and both the comonomer content and the molecular weight. The lamellar thickness was determined from the identity period of the one-dimensional scattering function and from the analysis of the one-dimensional correlation function. The crystallinity and the volume of the crystalline unit cell were determined by wide-angle X-ray scattering. Some considerations are reported on the partial inclusion in the crystall cell of the $-CF_3$ groups and on the expulsion into the amorphous regions of the $-O(CF_2)_2CF_3$ groups.

Introduction

The phase diagram of poly(tetrafluoroethylene) (PTFE) shows, under atmospheric pressure, three crystal forms, in correspondence to the solid−solid transitions at 19 and 30 °C (phase II for t < 19 °C; phase IV for 19 °C < t < 30 °C; phase I for 30 °C < t < t_m,[1,2] t_m being the melting temperature of the polymer).

Form II exhibits a triclinic structure, containing polymer chains in a 13/6 helix or, more probably, an incommensurate helix conformation, while form IV shows a partially ordered hexagonal structure and 15/7 chains. Finally, phase I is characterized by a disordered, pseudo-hexagonal structure.[1,3−5]

The phase diagrams of perfluorinated copolymers of tetrafluoroethylene (TFE) were studied for the hexafluoropropene (HFP) comonomer,[6] and it was observed that the above PTFE homopolymer transitions are displaced toward lower temperatures, and furthermore, they appear as a single transition even at small HFP contents. Moreover, it was proposed that the side perfluoromethyl groups can be included as point defects in the crystalline phase.[7,8]

More recently, a conformational analysis was performed[9] on TFE copolymers containing different comonomers. The authors agree with the hypothesis that the $-CF_3$ groups can be included in the crystal, but they also suggest the exclusion from the crystal lattice of the $-OCF_3$ and $-OCF_2CF_3$ side groups in the perfluoroalkyl vinyl ether copolymers (PFA).

It is known that the HFP copolymer shows a lamellar morphology,[7,8] while no data are available on the argument for other perfluorinated copolymers.

In the present paper, an analysis is described of the lamellar superstructures of TFE random copolymers containing perfluoropropyl vinyl ether, $CF_3CF_2CF_2$-$OCF{=}CF_2$ (FPVE), perfluoromethyl vinyl ether, CF_3-$OCF{=}CF_2$ (FMVE), and HFP, carried out by small-angle X-ray scattering (SAXS). On the examined samples, the degree of crystallinity and the unit cell parameters were also determined by wide-angle X-ray scattering (WAXS).

Table 1. Comonomer Content, Melt Flow Index MFI, Volume Crystallinity Φ_{VOL}, and Melting Temperature t_m of the Examined Samples

sample	comonomer	mol % of comonomer	MFI[a] (g/10 min)	Φ_{VOL}	t_m[b] (°C)
SA1	FPVE	0.9	10.0	0.376	314
SA2	FPVE	1.5	11.0	0.352	310
SA3	FPVE	2.5	11.0	0.347	303
M1	FPVE-FMVE	3.9	12.8	0.316	291
M2	FPVE-FMVE	3.9	2.8	0.274	284
F1	HFP	10.1	15.3	0.283	251
F2	HFP	6.7	2.9	0.292	263

[a] Determined at 372 °C/5 kg. [b] Determined by differential scanning calorimetry.

Experimental Section

Samples. The copolymers examined in the present work were produced by emulsion polymerization in the Laboratories of AUSIMONT S.p.A., Bollate (Milano). Table 1 reports the comonomer content, the melt flow index (MFI), the volume percent of crystallinity, and the melting temperature of the samples. The MFI was adopted as an index inversely related to the molecular weight: actually, no other techniques could be used, owing to the insolubility of the copolymers even at high temperatures. The volume percent of crystallinity Φ_{VOL} was determined by WAXS, as described below.

The samples SA1−3 are TFE-FPVE copolymers having a comparable molecular weight, but a different FPVE percent; F1 and F2 are TFE-HFP copolymers which differ both in the molecular weight and in the HFP content; finally, M1 and M2 are TFE-FPVE-FMVE terpolymers showing a constant total concentration of comonomers and different molecular weight.

Suitable specimens for WAXS, SAXS, and density measurements were prepared by compression molding of the granules, according to the ASTM D 3307-86 procedure. Finally, the densities were determined by following the ASTM D 792 method.

Wide-Angle X-ray Scattering. WAXS patterns were recorded in the diffraction angular range 5−50° (2θ) by a Seifert MZ III powder diffractometer equipped with a graphite curved-crystal monochromator on the diffracted beam; Cu Kα radiation was employed.

[⊗] Abstract published in *Advance ACS Abstracts,* February 15, 1996.

0024-9297/96/2229-2197$12.00/0

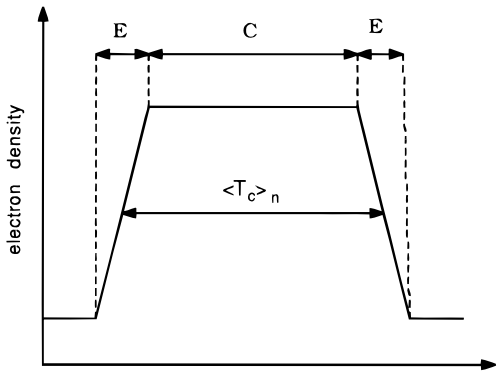

Figure 1. Electron density profile in a direction perpendicular to the lamellae for a pseudo-two-phase model.

The application of the least-squares fit procedures elaborated by Hindeleh and Johnson[10] gave the crystallinities by weight Φ of the samples, and the volume crystallinities were then evaluated by the equation:

$$\Phi_{VOL} = 1/\left(1 + \frac{1-\Phi}{\Phi}\frac{d_c}{d_a}\right) \quad (1)$$

where the crystal density $d_c = 2.302$ g/cm^3 and the amorphous one $d_a = 2.0$ g/cm^3.[11]

The hexagonal unit cell parameter a was evaluated from the experimental 2θ angular position of the *100* WAXS peak ($2\theta = 18°$). The relative error was estimated as 0.2% for a.

Small-Angle X-ray Scattering. The SAXS patterns were recorded by a Kratky camera, utilizing the Cu Kα radiation from a Philips PW 1830 X-ray generator. The data were collected by a MBraun OED-50-M position sensitive detector, in the scattering angular range 0.1−5.0° (2θ), and they were corrected for the blank scattering. A constant continuous background[12] was then subtracted, and the obtained intensity values $\tilde{I}$ were smoothed, in the tail region, with the aid of the $s\tilde{I}(s)$ versus $1/s^2$ plot.[13] Then the Vonk's desmearing procedure[14] was applied, and the one-dimensional scattering function was evaluated by the Lorentz correction: $I_1(s) = 4\pi s^2 I(s)$, where $I_1(s)$ is the one-dimensional scattering function and $I(s)$ is the desmeared intensity function, being $s = (2/\lambda)\sin\theta$.

The sum of the average thicknesses of the crystalline and amorphous layers was determined as the Bragg identity period D_B of the $I_1(s)$ function; the average lamellar thickness was calculated, for an ideal two-phase model, by the relation:[15] $C_B = D_B\Phi_{VOL}$.

A pseudo-two-phase model was also considered, where a transition layer E (Figure 1) is present and can be represented by a linear variation of the electron density between the crystalline core C and the amorphous layer. Vonk[13] showed that the tail region of the smeared scattering intensity can be fitted by the equation:

$$\tilde{I}(s) = (\pi k/2)(1/s^3 - 2\pi^2E^2/3s) \quad (2)$$

where k is a constant. In the plot of $s\tilde{I}(s)$ versus $1/s^2$, the slope is $\pi k/2$ and the intercept on the $\tilde{I}(s)$ axis is $\pi^3kE^2/3$: this allows us to evaluate the transition layer thickness E.[13]

The number average of the lamellar thickness $\langle T_c\rangle_n$ (Figure 1) was provided by the one-dimensional correlation function:[16]

$$\gamma_1(x) = \frac{\int_0^\infty s\tilde{I}(s)[J_0(2\pi xs) - (2\pi xs)J_1(2\pi xs)]\,ds}{\int_0^\infty s\tilde{I}(s)\,ds} \quad (3)$$

where J_0 and J_1 are zero- and first-order Bessel functions and x is the direction of the lamellar stacking. $\langle T_c\rangle_n$ was obtained by the relation:[12]

$$\langle T_c\rangle_n = B + (E/3)\Phi_{VOL}/(1-\Phi_{VOL}) \quad (4)$$

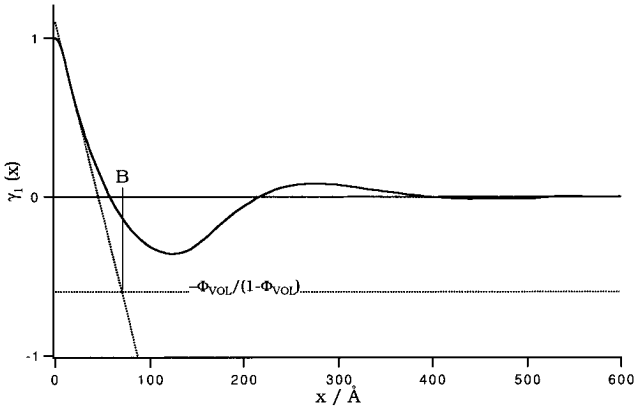

Figure 2. One-dimensional correlation function of the SA1 sample.

where B is the projection on the x axis of the intercept of the tangent to the linear region of $\gamma_1(x)$ with the horizontal line $\gamma_1(x) = -\Phi_{VOL}/(1-\Phi_{VOL})$. Figure 2 shows an example of this procedure, applied to the SA1 pattern. Since the γ_1 functions do not show a horizontal region in the first minimum, it was not possible to evaluate the crystallinities of the samples by SAXS.[12]

Finally, the crystalline core thickness C was calculated from $C = \langle T_c\rangle_n - E$ (Figure 1). The standard deviations of the $\langle T_c\rangle_n$, E, and C values are respectively 2%, 20%, and 5%, estimated by applying different fitting ranges in the linear region of $\gamma_1(x)$ and in the tail region of the $s\tilde{I}(s)$ versus $1/s^2$ plot.

Results and Discussion

The data reported in Table 1 point out, in all the examined samples, a similar trend as concerns the decrease of Φ_{VOL} by increasing both the comonomer content and the molecular weight. The comonomer insertion clearly gives rise to a break in the chain regularity, and hence it represents a hindrance to an ordered macromolecular packing; moreover, the presence of macromolecules having high molecular weight represents a further hindrance to the chain arrangement along regular structures (see also the melting temperature values in Table 1).

These effects are clearly detected in samples SA1−3, where an increase of FPVE from 0.9% to 2.5% gives rise to a decrease of the degree of crystallinity from 37.6% to 34.7%. The samples M1 and M2, containing the same total percent of FPVE and FMVE, show a crystallinity decrease at decreasing MFI, i.e., at increasing of the molecular weight. Finally, it can be noted that, in the HFP copolymers, the higher molecular weight of F2 is partially counterbalanced by the lower comonomer percent: as a matter of fact, the crystallinity of this sample is higher of less than one percent if compared to F1, in spite of the lower HFP content (6.7% in F2, 10.1% in F1).

The SAXS patterns of all the examined perfluorinated copolymers (Figures 3−5) present an evident maximum, which is typical of the two-phase lamellar structures: this confirms both the literature data for the TFE-HFP copolymers[7,8] and the presence of lamellar superstructures in the TFE-PFA copolymers.

Table 2 shows a decreasing trend of the long period D_B by increasing the comonomer percent in the sample SA1−3, while for M1 and M2 the increase of molecular weight gives rise to an increase of D_B. Finally, the increase of the lamellar periodicity, observed for F2, if compared to F1, can be associated to the parallel effects due to the decrease of the HFP content and the increase of the molecular weight. The values of the transition

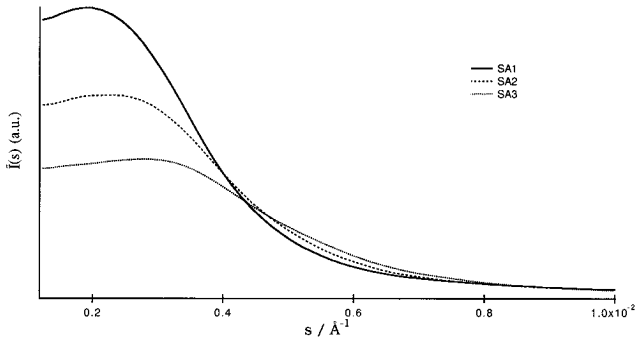

Figure 3. Experimental scattering functions of the examined SA1−3 samples.

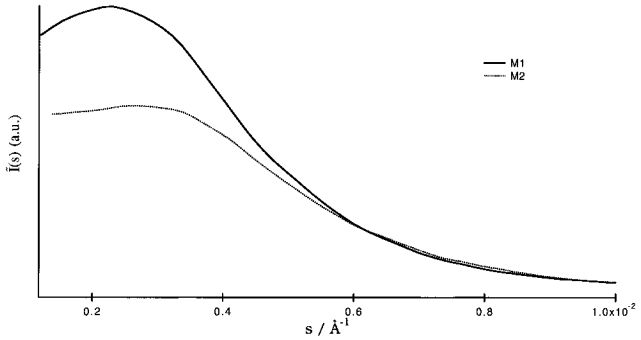

Figure 4. Experimental scattering functions of the examined M1 and M2 samples.

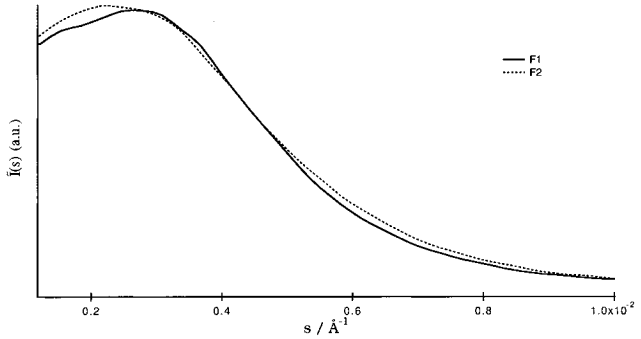

Figure 5. Experimental scattering functions of the examined F1 and F2 samples.

Table 2. Identity Period D_B, Lamellar Thicknesses C_B and $\langle T_c \rangle_n$, Crystalline Core Thickness C, Transition Layer Thickness E, and Crystal Unit Cell Parameter a of the Examined Samples

sample	D_B (Å)	C_B (Å)	$\langle T_c \rangle_n$ (Å)	C (Å)	E (Å)	a (Å)
SA1	297	112	81	70	11	5.66
SA2	261	92	69	58	11	5.68
SA3	233	81	61	50	11	5.66
M1	251	79	49	40	9	5.64
M2	261	72	48	37	11	5.70
F1	225	64	47	35	12	5.75
F2	251	73	54	41	13	5.75

layer thicknesses, reported in Table 2, do not depend on the molecular weight and on the comonomer percent; by considering that the transition layer represents a region where the polymer chains fold, it can be concluded that rigid macromolecules, like those considered in the present work, find only limited opportunities for varying the folding conditions.

As concerns the comparison between the lamella thickness values C_B and $\langle T_c \rangle_n$, it can be observed that the first ones are always larger. Since D_B is a weight-average value, the kind of average represented by C_B can be only defined if the Φ_{VOL} distribution over the lamellar stacks is known: if Φ_{VOL} is constant for all the lamellar stacks, then C_B is a weight-average[15] value, and under this condition the $C_B/\langle T_c \rangle_n$ ratio should be considered as representative of the polydispersion of the lamellar thicknesses. However, since no experimental evidences can be found to confirm this hypothesis, the overestimation of the lamella thickness evaluated by C_B is probably due, at least partially, to the lamellar morphology, which is not satisfactorily described by the ideal two-phase model, while the correlation function approach is valid for any pseudo-two-phase structure.[12,17,18]

The increase of the FPVE content in the SA1−3 samples gives rise to a decrease of the lamella thickness (C_B or $\langle T_c \rangle_n$) and of the crystalline core thickness C, in parallel with the above-described D_B value decrease (Table 2). A general trend is evident to exclude the comonomer from the crystalline lamellar regions during the crystallization process.

For the M1 and M2 samples, by decreasing the C value, it is observed in M2 (having a higher molecular weight) an increase of the long period D_B: in this case it can be concluded that an increase of molecular weight gives rise to a parallel increase of the amorphous region thickness, since the longer chains cannot fold in a lamellar organization, probably in consequence of the entanglement effect.

In spite of the higher molecular weight, compared to the F1 sample one, F2 shows an increase of C and a strong influence is observed also in this case of the comonomer percent on the lamellar thickness. However, the accompanying effects of both the molecular weight increase and HFP content do not allow a comparison of the results with those obtained for the PFA copolymers.

By considering that the value of the parameter a of the hexagonal unit cell of PTFE, reported in the literature, is 5.66 Å,[19,20] a significant deviation can be noted in Table 2 of this value if compared to the corresponding parameters determined by WAXS for F1 and F2. The distortion of the unit cell demonstrates that the $-CF_3$ group is at least partially included into the crystalline phase, differently from the more cumbersome $-O(CF_2)_2CF_3$ side group, whose corresponding unit cell does not show distortion effects. This is in agreement with the results of a conformational analysis performed on analogous copolymers.[9]

Conclusions

The present investigation put into particular evidence the lamellar morphology of TFE copolymers with FPVE and FMVE: the introduction of small comonomer percents (0.9% of FPVE in SA1) gives rise to a change from an extended chain conformation, typical of PTFE, to the lamellar morphology which was previously reported for some TFE-HFP copolymers.

Finally, it is interesting to underline that the joined application of SAXS and WAXS techniques allowed us to ascertain that the $-CF_3$ side groups can be at least partially included into the crystal unit cell, giving rise to an expansion of the same, while on the contrary the $-O(CF_2)_2CF_3$ group is expelled into the amorphous regions through a decrease of the lamellar thickness.

Acknowledgment. The authors thank the MURST (Ministero per l'Università e la Ricerca Scientifica e Tecnologica) of Italy for financial support and the CUGAS (Centro Universitario Grandi Apparecchi Sci-

entifici) of the University of Padua for making available the SAXS instrumentation.

References and Notes

(1) Bunn, C. W.; Howells, E. R. *Nature (London)* **1954**, *174*, 549.
(2) Sperati, C. A.; Starkweather, H. W. *Adv. Polym. Sci.* **1961**, *2*, 465.
(3) Clark, E. S. *Bull. Am. Phys. Soc.* **1962**, *18*, 317.
(4) Corradini, P.; Guerra, G. *Macromolecules* **1977**, *6*, 1410.
(5) Weeks, J. J.; Clark, E. S.; Eby, R. K. *Polymer* **1981**, *22*, 1480.
(6) Weeks, J. J.; Sanchez, I. C.; Eby, R. K.; Poser, C. I. *Polymer* **1981**, *21*, 325.
(7) Eby, R. K. *J. Res. Natl. Bur. Stand. (U.S.)* **1964**, *Sect. A 68*, 269.
(8) Bolz, L. H.; Eby, R. K. *J. Res. Natl. Bur. Stand. (U.S.)* **1965**, *Sect. A 69*, 481.
(9) Villani, V.; Pucciariello, R.; Fusco, R. *Colloid Polym. Sci.* **1991**, *269*, 477.
(10) Hindeleh, A. M.; Johnson, D. J. *J. Phys. (D)* **1971**, *4*, 259.
(11) Starkweather, H. W.; Zoller, P.; Jones, G. A.; Vega, A. J. *J. Polym. Sci., Part B: Polym. Phys.* **1982**, *20*, 751.
(12) Vonk, C. G.; Pijpers, A. P. *J. Polym. Sci., Part B: Polym. Phys.* **1985**, *23*, 2517.
(13) Vonk, C. G. *J. Appl. Crystallogr.* **1973**, *6*, 81.
(14) Vonk, C. G. *J. Appl. Crystallogr.* **1971**, *4*, 340.
(15) Vonk, C. G. *Makromol. Chem., Macromol. Symp.* **1988**, *15*, 215.
(16) Vonk, C. G. *Synthetic Polymers in the Solid State in Small Angle X-ray Scattering*; Glatter, O., Kratky, O., Eds.; Academic Press: London, 1982; p 433.
(17) Strobl, G. R.; Schneider, M. J. *J. Polym. Sci., Part B: Polym. Phys.* **1980**, *18*, 1343.
(18) Defoor, F.; Groeninckx, G.; Reynaers, H.; Schouterden, P.; Van der Heijden, B. *Macromolecules* **1993**, *26*, 2575.
(19) Clark, E. S.; Muus, L. T. *Z. Kristallogr.* **1962**, *117*, 119.
(20) Marega, C.; Marigo, A.; Garbuglio, C.; Fichera, A.; Martorana, A.; Zannetti, R. *Makromol. Chem.* **1989**, *190*, 1425.

MA950809+